Proceed. Int. AMSE Conf. "Modelling & Simulation", Monastir, Nov. 25-28, 1985, p. 137-146
Vol. 2A

'ZOMBIE', A COUPLED PROCESS-DEVICE-SIMULATOR

W.Jüngling, P.Pichler, S.Selberherr, H.Pötzl
Institut für Allgemeine Elektrotechnik und Elektronik
Technical University of Vienna
Gußhausstr.27-29, 1040-Vienna, AUSTRIA

Abstract - The miniaturization of electronic devices requires improved physical models and numerical methods to keep pace with new process techniques. To cover these demands we have developed the coupled process- device-simulator ZOMBIE. This program permits the easy implementation of complicated physical models and provides a secure numerical environment for the evaluation. A complete simulation of a n^+-p-p^+ diode fabrication step and the simulation of the electric characteristic are presented. The numerical background is outlined and explained by the examples.

Introduction

The process and device simulation of miniaturized electronic devices requires the use of improved physical models. The complicated models often burst the capabilities of existing process simulators. Furthermore, they need a secure numerical environment since critical steps during the simulation can often not be estimated in advance. This situation incited us to create the simulator ZOMBIE which permits easily the evaluation of complicated physical models. The models are implemented just by specifying their most important functions (Eq.(4a-g)). The discretization and the linearization are performed by the program. Many numerical problems which result in laborious work like grid generation in space and time are performed without any user interaction. The user can therefore concentrate on the physical model itself. Critical simulation domains in space and time are detected automatically and carefully resolved.

The program ZOMBIE is mainly used for the development of new process and device models. The presented strategies for the secure numerical environment are also of interest for the development of two- or three-dimensional simulators since they reduce the amount of required memory and CPU-time.

The Physical Models for Simulation

ZOMBIE handles a coupled system of an arbitrary number 'n' of partial differential equations described by Eq.(1) and Eq.(2) and the boundary conditions denoted by Eq.(3). The equations consist of a general continuity equation

$$\sum_{j=1}^{n} \alpha_{ij} \frac{\partial C_j}{\partial t} + \frac{\partial J_i}{\partial x} = G_i \qquad (1)$$

and a general flux relation

$$J_i = \sum_{j=1}^{n} D_{ij} \cdot \frac{\partial C_j}{\partial x} + \sum_{j=1}^{n} \mu_{ij} \cdot C_j \cdot \frac{\partial \Psi}{\partial x} \qquad (2)$$

where Ψ, the potential, is one of the variables C_i, i=1,n.

The boundary conditions can be written as

$$\sum_{j=1}^{n} \xi_{ij} \cdot C_j + \sum_{j=1}^{n} \eta_{ij} \cdot J_j = F_i \qquad (3)$$

The implementation of a model requires only the specification of the functions:

$$\alpha_{ij} = \alpha_{ij}(x,t) \qquad (4.a)$$
$$G_i = G_i(x,t,C_k,J_m) \qquad (4.b)$$
$$D_{ij} = D_{ij}(x,t,C_k,J_m) \qquad (4.c)$$
$$\mu_{ij} = \mu_{ij}(x,t,C_k,J_m) \qquad (4.d)$$
$$\xi_{ij} = \xi_{ij}(x,t) \qquad (4.e)$$
$$\eta_{ij} = \eta_{ij}(x,t) \qquad (4.f)$$
$$F_i = F_i(x,t,C_k,J_m) \qquad (4.g)$$

with i,j,k,m = 1..n.

This system of differential equations permits the simulation of e.g. semiconductor equations, standard process steps, the Poisson equation, the growth and shrinkage of stacking faults or the simulation of the point defect kinetics during the oxidation. The variables C_i are not restricted to concentrations but can represent potentials, or, for instance, the length of stacking faults or the radii of precipitates. The discretization and linearization of the models requires no further user interaction and is done automatically by the program.

Process Simulation

The process steps for the fabrication of the n^+-p-p^+ diode are chosen to obtain critical simulation steps. Fig.1 specifies the process parameters and shows the process temperatures as a function of time. The starting material is a $10^{15}cm^{-3}$ boron doped wafer with a thickness of 50μm. Arsenic is implanted through the surface at the lower boundary. During the second annealing step the p-contact fabrication is simulated by a boron predeposition at the upper boundary. The high dose arsenic implantation requires the use of a dynamic arsenic clustering model, since the solubility limit of the arsenic is exceeded at all process temperatures.

The improved model requires the simulation of the clustered arsenic concentrations which lead to an additional quantity during the simulation. We use the cluster model proposed by /1/. The physical model is summarized in Eq.(5) to Eq.(10).

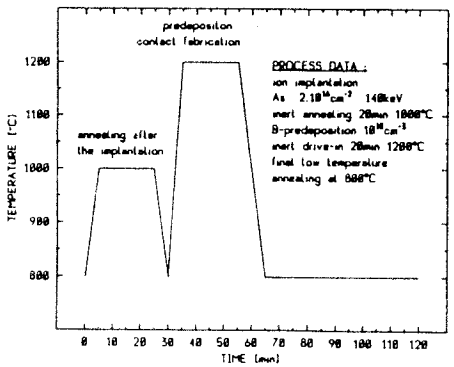

Fig.1

$$\frac{\partial C_{As}}{\partial t}=\mathrm{div}(D_{As}\cdot \mathrm{grad}C_{As}+C_{As}\cdot\mu_{As}\cdot\mathrm{grad}\Psi)+k_D\cdot C_{Cl}-k_C\cdot C_{As}^{m}\cdot n^{k} \qquad (5)$$

$$m\cdot\frac{\partial C_{Cl}}{\partial t}= -k_D\cdot C_{Cl}+k_C\cdot C_{As}^{m}\cdot n^{k} \qquad (6)$$

with m=3 and k=1.

$$\frac{\partial C_B}{\partial t}=\mathrm{div}(D_B\cdot\mathrm{grad}C_B-C_B\cdot\mu_B\cdot\mathrm{grad}\Psi) \qquad (7)$$

$$\Psi = U_t\cdot\mathrm{arsinh}\left(\frac{C_{As}+(m-k)\cdot C_{Cl}-C_B}{2\cdot n_i}\right) \qquad (8)$$

The electric potential is computed by the quasineutral assumption which turns out to be a sufficiently good approximation for the solution of the exact Poisson equation /2/.

The boundary conditions during the inert annealing steps are summarized in Eq.(9) to Eq.(10).

$$J_{As}(x=0\mu m)=0 \quad J_{As}(x=50\mu m)=0 \quad J_B(x=0\mu m)=0 \quad J_B(x=50\mu m)=0 \qquad (9)$$

$$J_{As}(x=0\mu m)=0 \quad J_{As}(x=50\mu m)=0 \quad J_B(x=0\mu m)=0 \quad C_B(x=50\mu m)=10^{18}cm^{-3} \qquad (10)$$

In the beginning we assume all arsenic to be electrically active. Fig.2A shows the arsenic concentration after the ion implantation, Fig.2B after the first 1000°C annealing step. The comparison between the figures shows the spreading of the arsenic profile as well as the transformation from electrically active arsenic into clustered arsenic.

Fig.2C and Fig.2D show the final distribution of the dopants at both boundaries. The use of an arsenic cluster model is necessary since the maximum solubility of arsenic is exceeded during all process steps. Fig.3 shows the transformation from active into clustered arsenic and back. The figure shows that equilibrium is not obtained during the process steps and that a dynamic cluster model is necessary to obtain accurate results.

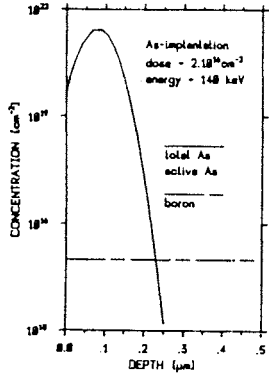

Fig.2A

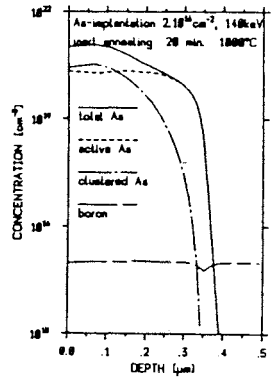

Fig.2B

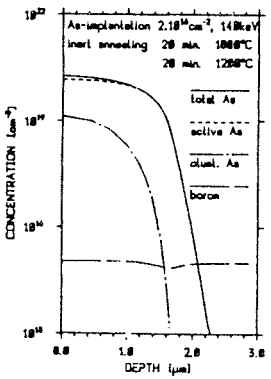

Fig.2C

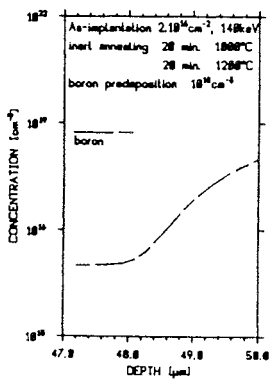

Fig.2D

The two process steps include very critical simulation domains. The spreading of the steep arsenic profile requires a fine resolution in the vicinity of the p-n junction. The boron predeposition needs a very accurate resolution in the very beginning of the contact fabrication. Rigid grids in space and time can by no means fulfil all the requirements without using enormous memory resources. Using rigid problem-oriented grids requires the knowledge of the solution in advance to optimally position the grid points and time steps. Fully adaptive grids in space and time are therefore implemented into ZOMBIE. Fig.4A-B-C show the grid modifications during the most important process steps. The lines in the Fig.4A-B-C show existing grid points during the simulation. A beginning or terminating gridline indicates a new or a deleted gridpoint. Fig.4A shows the grid modifications during the first 35min. The grid indicates the spreading of

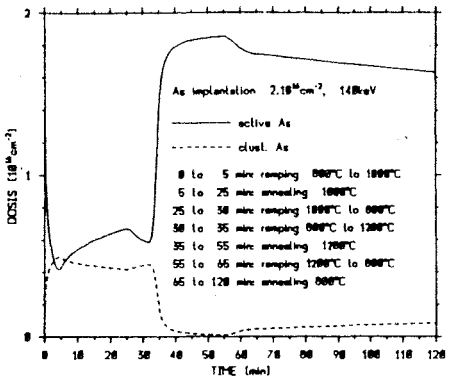

Fig.3

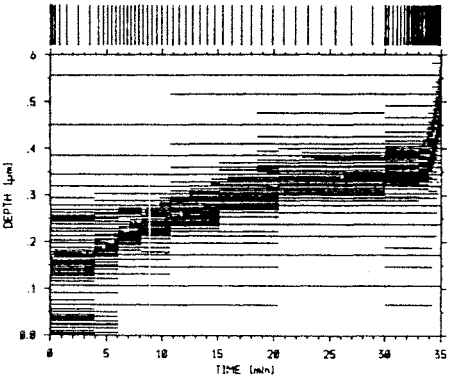

Fig.4A

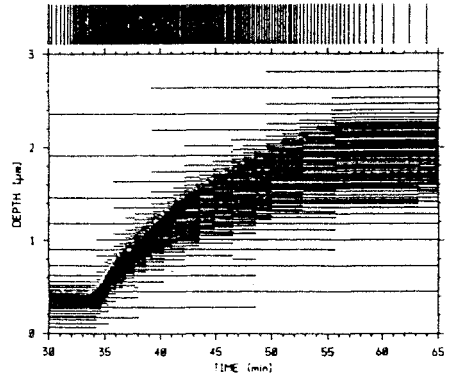

Fig.4B

the arsenic profile during the 1000°C temperature step and the beginning of the 1200°. The vertical bars at the top of the Fig.4A-B-C show the transient grid used for the simulation. Fig.4A and Fig.4B show the advantages of the adaptive transient grid. Very critical simulation domains e.g. the high temperature annealing are clearly resolved whereas low temperature processes are simulated with larger time steps. Fig.4C shows the grid evolution at the upper boundary during the boron predeposition. Many gridlines are inserted in the beginning and removed afterwards.

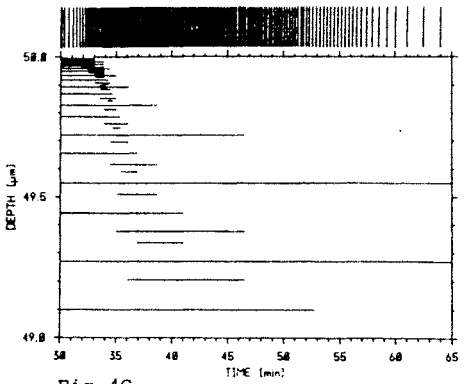

Fig.4C

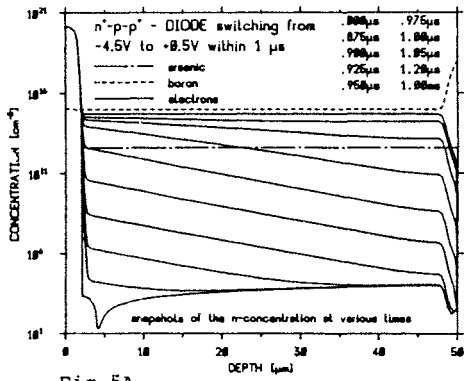

Fig.5A

Device Simulation

The n^+-p-p^+ diode which has been simulated in the last chapter will be used for the device simulation with ZOMBIE. We present the simulation of the +0.5V forward biased diode, the -4.5V reverse biased diode as well as the switching between the two states. Fig.5A-B-C and

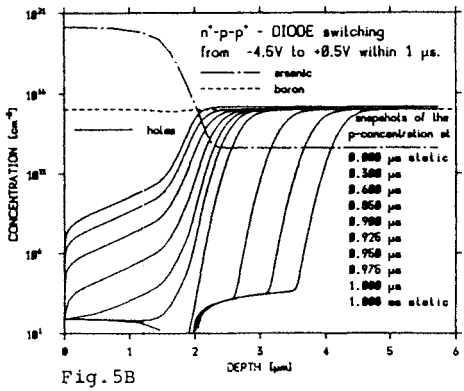

Fig.5B

Fig.6A-B-C show the electron concentration, the hole concentration and the grid modifications during the switching-on and the switching-off. The vertical bars on the top of the figures indicate the transient mesh used for the simulation of these processes. Fig.5A shows the electron concentration in the whole simulation domain during the switching-on. The distribution during the reverse bias and the injection of electrons from the n^+-domain into the p-domain are plotted. Fig.5B shows the hole concentrations during the switching-on in the vicinity of the p-n junction and shows the reduction of the space charge layer with increasing external voltage. Fig.5C shows the corresponding grid modifications. The reverse bias requires a fine resolution close to the boundaries of the space charge layer, the forward bias a fine resolution in the vicinity of the contacts. The transient integration requires a fine

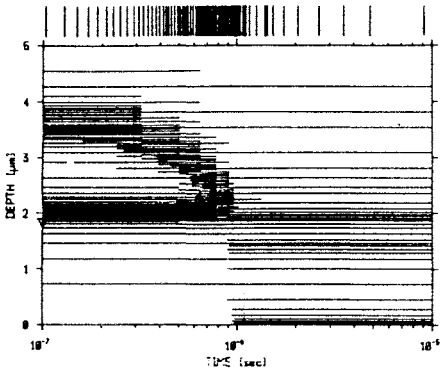

Fig.5C

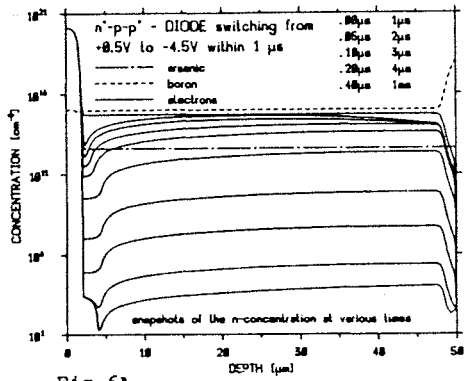

Fig.6A

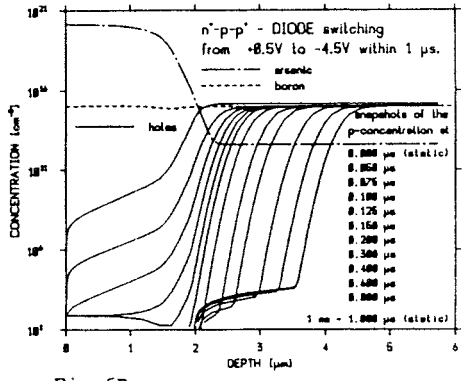

Fig.6B

resolution during the transition from the reverse to the forward bias (i.e. at 0.9µs in this example). Fig.6A shows the electron concentrations during the switching-off and the creation of the space charge layer. The grid modifications are plotted in Fig.6C and show the formation and enlargement of the space charge layer.

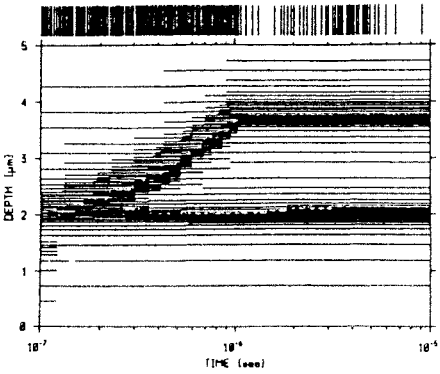

Fig.6C

How to Create Adaptive Grids

The strategies for the generation and modification of grids must be independent from the physical model under consideration. The design of a spatial grid can be split up into two independent parts. Computation of the position of the maximum discretization error and refinement of the grid in the vicinity of this position /3/. The computation of the discretization error depends on the discretization method, e.g. finite differences, finite boxes or finite elements. We use the methods of finite differences and therefore the deviation of the distribution of the variables from a local polynomal of second order can be taken as a measure of the spatial discretization errors. The computation of the discretization error should be insensitive to slight truncation errors and the discretization error should decrease with decreasing mesh spacing. (The use of numerical differentiation should be avoided therefore). All criteria which fulfil these demands may be used and will lead to similar spatial grids.

A quasiuniform spatial mesh can be recommended for all simulations and should be kept during all grid modifications /4/. A mesh is called quasiuniform if the ratio between two adjacent grid spacings minus unity is small compared to unity. This mesh avoids abrupt transitions from a very coarse to a very fine mesh.

Furthermore, the discretization error decreases with the square of the mesh spacing. We use the "sectio aurea" for the grid refinement, e.g. h_i/h_{i-1}=sqrt(1.25)+0.5, 1 or sqrt(1.25)-0.5. Fig.7 compares a quasiuniform mesh to an arbitrary mesh. (The sectio aurea holds AB:BC=BC:CD and AB=BD). It should be noted that a quasiuniform mesh often requires the modification of a larger grid domain. In our example the points C and E must be inserted together. To remove grid points is more difficult than to insert grid points. Therefore, we prefer the generation of a completely new grid after a certain number of additional grid points have been inserted or after a certain number of time steps have elapsed.

For the transient integration we use "backward difference formulae" of 6^{th} order /5/,/6/. This method permits the exact integration of polynomals of 6^{th} order. The comparison of a predicted with a computed solution permits the detection of critical simulation domains, the step width control and the order control.

The large dynamic range of the semiconductor equations and the process variables permits a relative error control only. We check the error of every variable at every depth. The maximum error between the predicted and the computed solution determines the step width for the next iteration. The step width is computed for the actual order and the order minus and plus one. The order which permits the largest time step is chosen for the next iteration. If the error exceeds a limit the time step is rejected and the simulation is repeated with a smaller time step.

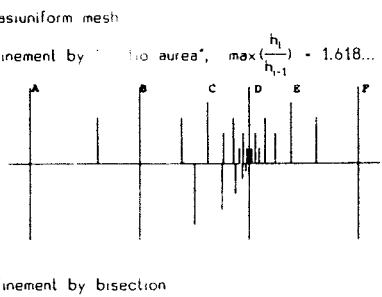

Fig.7

Summary

We have presented results of critical process and device simulations using the program ZOMBIE. The simulator supports fully adaptive spatial and transient grids. The adaptive spatial grid reduces the memory requirements by a factor of up to 20 during process simulations and up to 5 during device simulations. The additional CPU-time used for the grid modifications is about 10% of the simulation time and by far compensated by the reduction of time during the solution of the partial differential equations with decreased number of gridlines. The fully adaptive grid in time saves additional CPU-time.

A fully adaptive grid is important for process and device simulations in two ways. Firstly, it enables the development of new models for process and device simulations, because it frees the user from nearly all mathematical considerations about grid generation and step width control during the simulation. Secondly, it reduces the CPU-time and memory requirements of the simulation which is particulary important with two- or three-dimensional simulations.

Acknowledgements - This work has been sponsored by SIEMENS Research Laboratories, Munich, W.Germany and the Fonds zur Förderung der Wissenschaftlichen Forschung Proj.S43/10.

References

/1/ Tsai M.Y.,Morehead F.F.,Baglin J.E.E., "Shallow Junctions by High-Dose As Implants in Si: Experiments and Modeling",J. Appl. Phys.,Vol.51,6,pp.3230-3235,June 1980

/2/ Jüngling W.,Pichler P., Selberherr S., Guerrero E., Pötzl H., "Simulation of Critical IC-Fabrication Processes Using Advanced Physical and Numerical Methods", IEEE-SSC Vol.SC-20, No.1, Feb.1985

/3/ Pichler P., Jüngling W., Selberherr S., Guerrero E., Pötzl H., "Simulation of Critical IC-Fabrication Processes", in print (IEEE-ED, Oct.1985)

/4/ Selberherr S., "Analysis and Simulation of Semiconductor Devices", Springer Verlag Wien-NewYork, 1984, ISBN 3-211-81800-6

/5/ Brayton R.K., Gustavson F.G., Hachtel G.D., "A New Effective Algorithm for Solving Differential-Algebraic Systems Using Implicit Backward Differentiation Formulas", Proc.IEEE, Vol.60, pp.98-108, 1972

/6/ Gear C.W., "The Automatic Integration of ordinary differential Equations", Information Processing 68, North Holland, 1968, pp.187-193